ELSEVIER

Journal of Nuclear Materials 299 (2001) 148–156

journal of nuclear materials

www.elsevier.com/locate/jnucmat

Varying temperature irradiation experiment in HFIR

T. Muroga [a,*], S.J. Zinkle [b], A.L. Qualls [b], H. Watanabe [c]

[a] National Institute for Fusion Science, 322-6 Oroshi, Toki, Gifu 509-5292, Japan
[b] Oak Ridge National Laboratory, P.O. Box 2008, Oak Ridge, TN 37831-6138, USA
[c] Research Institute for Applied Mechanics, Kyushu University, Kasuga, Fukuoka 816-8580, Japan

Received 7 June 2001; accepted 5 August 2001

Abstract

Post-irradiation examination has started and initial results are available for the varying temperature irradiation experiment conducted in the high flux isotope reactor (HFIR), carried out in the framework of the Japan–USA Fusion Cooperation Program (JUPITER project). This experiment is an unprecedented controlled irradiation experiment designed for symmetrical comparison of isothermal and temperature-variant neutron irradiation effects. This paper summarizes the irradiation experiments and initial results obtained from the post-irradiation examination of an austenitic alloy, vanadium, a vanadium alloy and copper. These preliminary results extend the trends observed in earlier, lower fluence experiments, with some effects of the low temperature phase of variable temperature irradiation on evolving microstructures.

1. Introduction

Numerous experiments have demonstrated that temperature transient during irradiation can have a strong impact on the response of materials [1–24]. The comparison of conventional (with some variation) and controlled temperatures during operation of Japan materials testing reactor (JMTR) [2–5] and the observation and analysis of defect clusters formed during the shutdown procedure of fast flux test facility (FFTF) [6–9] strongly suggested the need for carefully controlled temperature-variant irradiation experiments. The major motivation for such experiments is to reexamine the previously obtained neutron irradiation data taking the temperature transient effects into account and to predict performance of fusion structural materials subject to temperature variation during operation [9].

Fundamental studies of the effects of temperature transients during irradiation have been performed by intentional temperature changes during irradiation or by re-irradiation at different temperatures. These studies have used neutrons [10–15], heavy ions [16–22] and electrons [23,24]. In particular, systematic low dose fission neutron irradiation experiments with and without intentional temperature variation have been carried out in JMTR [11–15]. These studies showed the influence of the temperature excursion varied from negligible to strong, depending on the temperature range, variation period and frequency, as well as on the materials.

The JMTR research was focused mainly on microstructure evolution at low dose levels (~0.1 dpa) because of the limitation on flux and irradiation volume.

Rate theory and kinetic Monte Carlo analyses of defect accumulation, microstructural evolution and mechanical property change have been carried out for varying temperature irradiation conditions [25–28]. These studies have been aimed at understanding the existing data and at predicting the possible temperature change effects on the performance of materials in fusion conditions.

In the Japan–USA Fusion Cooperation Program (JUPITER project), a 'Varying Temperature Irradiation Experiment' was selected as one of the major collaboration tasks [29]. The experiment is complementary to the irradiation studies with JMTR in extending the dose level (~0.1 dpa in JMTR and ~5 dpa in HFIR). The

* Corresponding author. Tel.: +81-572 58 2314; fax: +81-572 58 2676.
E-mail address: muroga@nifs.ac.jp (T. Muroga).

0022-3115/01/$ - see front matter
PII: S0022-3115(01)00675-4

experiment also includes mechanical property measurements using various small size specimens.

2. Outline and progress of the experiment

The history of the varying temperature irradiation experiment is summarized in Fig. 1. The design of the experiment progressed through phases of technical assessment, conceptual design and engineering design. During the engineering design, mock-up tests were carried out to verify the temperature control technique. The experimental design and fabrication, the specimens matrix and the operation of the experiment in the HFIR have been reported earlier in [30–35].

The capsule temperature control zones and the designed temperature control scenario are schematically shown in Fig. 2. The experiment has four irradiation zones; low temperature steady (Zone A – 350 °C), high temperature steady (Zone B – 500 °C), high temperature variable (Zone C – 300/500 °C) and low temperature variable (Zone D – 200/350 °C). In the variable zones, the temperatures were reduced for the initial 10% period of each irradiation cycle (low T phase), and elevated for the remaining 90% period (high T phase). Paired specimens were loaded symmetrically with respect to the reactor mid-plane in order to be subjected to a similar fluence and spectrum of neutrons.

Temperature control was carried out using a combination of the control of the gas composition (Ne or Ar, and He) in a thermal insulating gap between specimen holders and the capsule wall, and control to 8 electric heaters per specimen holder. Temperature monitoring was carried out using 28 thermocouples in total, which measured the temperature of each holder at distinct axial locations distributed angularly at three locations, and of 5 dummy specimens.

Four types of specimens were included in the experiment. They are transmission electron microscopy (TEM) discs, small size tensile specimens with gauge length of 5 mm, small size Charpy V-notch (CVN) specimens with dimensions 1.5 mm × 1.5 mm × 20 mm and bend-bar specimens with dimensions 1.0 mm × 0.7 mm × 10 mm. The specimens were contained in sleeves fitted in axial holes in the holders. The purpose of the sleeves is to position the specimens and to enhance the heat transfer from the specimens to the holder. Alumina dispersion strengthened aluminum (DISPAL) was chosen as the material for the holders and the sleeves because of its low nuclear heating rate, fair strength and fabricability and compatibility with various specimen materials. Fig. 3 shows tensile test specimens contained in a sleeve being loaded into a hole in the holder. Six of the specimen sleeves are shown in Fig. 3, occupying the large diameter holes. A number of smaller holes in the holders are for gas-lines, electric heaters and thermocouples.

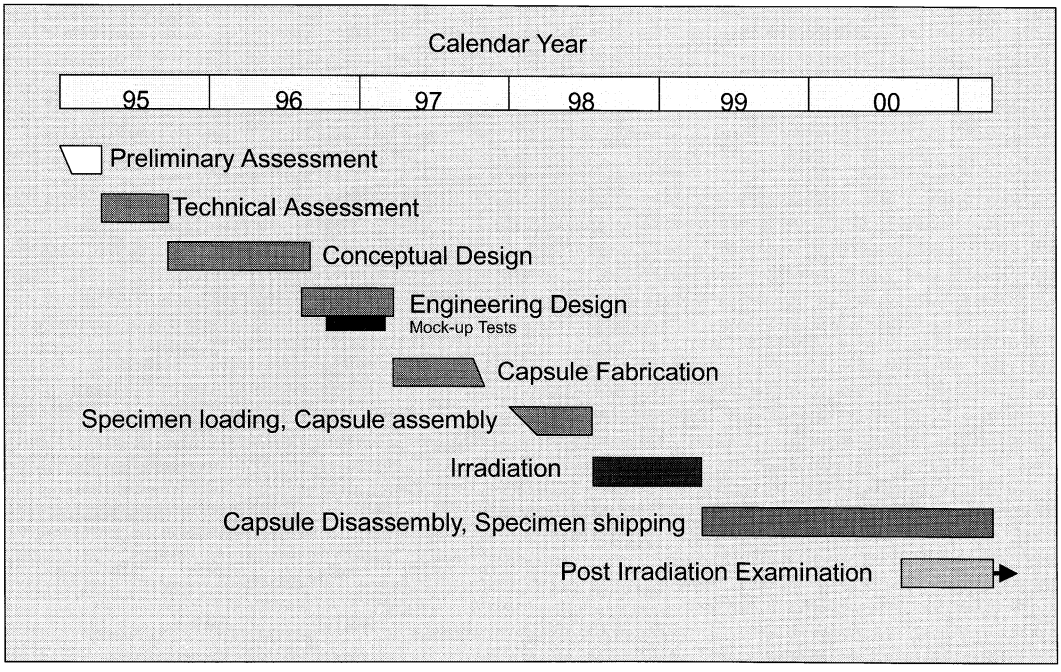

Fig. 1. History of the varying temperature irradiation experiment in HFIR under the Japan–US Fusion Cooperation Program (JUPITER project).

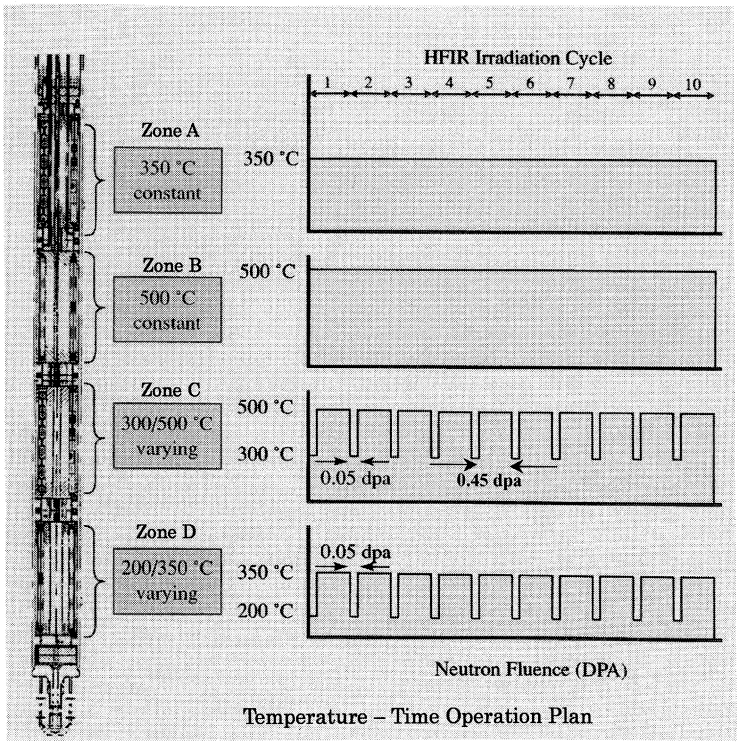

Fig. 2. The capsule temperature control zones and planned temperature control scenario for the varying temperature irradiation experiment.

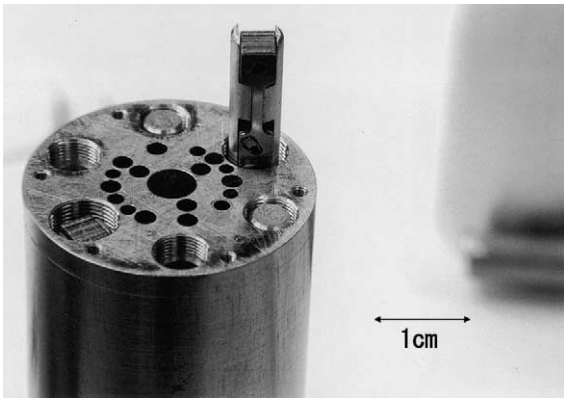

Fig. 3. A photograph taken when tensile specimens contained in a sleeve were being loaded into the holder.

Specimen materials irradiated in this experiment included low activation ferritic steels and their model alloys, model and candidate vanadium alloys, austenitic steels and their model alloys, copper and copper alloys, and others (Mo, W, Ni, Nb, Ta, Al and their alloys and some ceramics). About 1000 TEM discs, 350 tensile specimens, 50 CVN and 80 bend bars were loaded in each of the four zones. The irradiation was planned for 10 cycles in a europium shielded capsule in one of the Removable Beryllium (RB) positions of HFIR.

Irradiation of the varying temperature irradiation experiment started in HFIR on July 22, 1998 (Cycle 362) and ended on May 16, 1999 (Cycle 369). This was two cycles short of the planned ten-cycle operation, with capsule removed due to leakage in a gas supply line into the capsule. It operated 195.1 effective full power days (EFPDs), which roughly corresponds to 4 dpa for steels. Of the 32 heaters operating at the initiation of the irradiation, two heaters were removed from service because low electrical resistance from the element to ground was detected. All 28 thermocouples were operational during the experiment.

The indicated temperature, which is the average of 5 to 7 thermocouples installed into each zone, are shown in Fig. 4. The third cycle had a mid-cycle shutdown and restart. Three minor temperature excursion occurred during the operation. The average indicated temperatures and the estimated variation of the four zones are listed in Table 1. During operation, the average indicated temperatures were intended to be controlled 10 K below the nominal temperatures, to account for temperature difference between the holders and the specimens. In Zone B, however, the temperature could not be controlled at the design point because the nuclear heat-

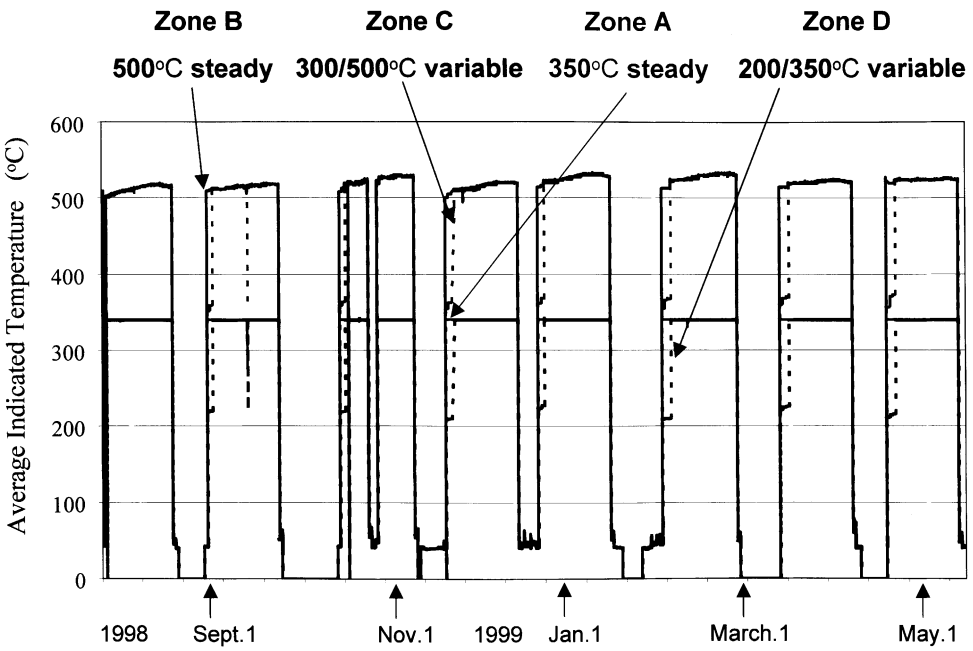

Fig. 4. Average indicated temperatures of the four zones for the full period of irradiation.

Table 1
The average indicated temperatures and their variation for the four zones

	Zone A	Zone B	Zone C		Zone D	
			Low T phase	High T phase	Low T phase	High T phase
Nominal temperature (°C)	350	500	300	500	200	350
Average indicated temperature (°C)	340	510	350	510	225	340
Temperature variation (°C) max/min	339/341	490/520	334/362	500/520	222/230	339/340
Estimated average specimen temperature (°C)	340	520	360	520	225	340

The data are extracted from histograms of readings from thermocouples taken at one-hour intervals during the irradiation. Temperature transients during the reactor start-up, reactor shut-down, the shift from the low T phase to high T phase, and the three minor temperature excursion events were not included in the statistics. Estimated specimen temperatures are also listed, which is derived by the measured specimen-to-holders temperature difference. The details are shown in [35].

ing rate was higher than predicted or the capsule gap thermal resistance was higher than expected. As a result, the holder temperature remained higher than the design point and changed with time as seen in Fig. 4. The temperature of Zone C during the high T phase was manually adjusted to keep it close to that of Zone B. Similar temperature deviation occurred during the low T phase of Zone C and Zone D. The average indicated temperatures were precisely controlled in Zone A for most of the time and Zone D during the high T phase as seen in Table 1. The goal temperature for the control was set 10° below the designed temperature, based on the calculation that the actual specimen temperature would be ~10 K above the holder temperature. Monitoring of thermocouples attached to dummy specimens showed that the temperature difference between the specimen and the holder varied from 8 to + 15° depending on the specimen shape, alloy and location, and irradiation cycle. Estimated average specimen temperature is also listed in Table 1. The details are reported in [35].

After irradiation the capsule was stored in the reactor water pool for about one year. This allowed decay of short lived radioactivity. It was then disassembled and the specimens were retrieved and shipped to hot laboratories. Some of the post-irradiation TEM examination started late 2000 at ORNL and PNNL.

Major technological developments accomplished in this experiment are summarized as follows:

1. Robust electrical heaters were developed which can withstand neutron irradiation to at least 4 dpa.
2. The procedure to maintain constant specimen temperatures, irrespective of the change in the reactor

power, was established using a combination of the control of the gas (mixture of Ne or Ar and He) composition in a thermal insulating gap between specimen holders and the capsule wall, and control to electric heaters.
3. The procedure to change specimen temperatures in a stepwise manner during irradiation was established, using a combination of the compositional control of the gap gas and power control to the electric heaters.
4. Accurate temperature evaluation was achieved by monitoring the temperature distribution in the holders and the temperatures of representative dummy specimens using 28 thermocouples in total.

3. Results of the initial post-irradiation examination

Microstructural examination using TEM has been carried out on specimen pairs which compare the symmetrical isothermal and temperature-variant irradiation conditions. This paper reports the results from Zones A and D, namely 340 °C constant and 225/340 °C variable (estimated average specimen temperature) irradiation. The materials were Fe–16Cr–17Ni austenitic ternary alloy, unalloyed V, V–4Cr–4Ti and unalloyed Cu. Fe–16Cr–17Ni alloy was melted from Johnson–Matthey high purity starting materials in a flowing pure hydrogen atmosphere and solution-treated at 1100 °C for 0.5 h. Unalloyed vanadium contained 13 ppm O, 60 ppm N, 120 ppm Fe, 40 ppm Si and 100 ppm Al, and annealed at 1100 °C for 2 h. V–4Cr–4Ti alloy contained 590 ppm O and 4 ppm N and annealed at 1100 °C for 2 h. Unalloyed copper, produced by arc melting, contained about 25 ppm O and annealed at 600 °C for 2 h. The materials used are from the same batch as those reported for Fe–16Cr–17Ni [11], unalloyed V [19], V–4Cr–4Ti [20] and unalloyed Cu [36].

Microstructural parameters obtained by the TEM are listed in Table 2. Other microstructural observations including specimens irradiated in the 360 °C constant and the 360/520 °C variable conditions are in progress. The results will be reported separately [37].

3.1. Fe–16Cr–17Ni austenitic alloy

Fig. 5 compares the microstructures under bright-field kinematical conditions for Fe–16Cr–17Ni induced by 340 °C steady and 225/340 °C variable irradiations. A low density of small cavities was observed in the variable case. The cavity density was much lower in the steady case. Fig. 6 shows the microstructure of the same specimens but in a dark-field weak-beam condition. Dislocation loops and small defect clusters, most of which were identified to be stacking fault tetrahedra (SFT) by their triangular shape when observed from $\langle 1\,1\,0\rangle$ directions, were observed in both specimens. The density of the clusters in the variable case was significantly lower than that in the steady case.

A suppression of defect evolution was reported for the same alloy irradiated in JMTR to 0.13 dpa with the periodic temperature change at 200/400 °C [11]. The suppression of defect evolution by the change of temperature was also confirmed by heavy ion irradiation of the same alloy to 1.4 dpa [18]. In those cases, evolution of all defects including loops, SFT and voids was retarded. In the present case, however, the density of SFT was selectively decreased by the temperature variation. Rate theory analyses showed that the accumulation of vacancy clusters during the lower temperature irradiation suppressed the dislocation evolution during the subsequent irradiation at a higher temperature [11,18]. However the model cannot explain the suppression of SFT by the temperature change as observed in the present study.

The cavity density of $\sim 10^{21}/m^3$ has been reported for model austenitic ternaries at ~400 °C [38,39], and higher density is expected at 340 °C based on the data compilation [40]. The much lower cavity density shown in Table 2 implies that the cavity nucleation was still in the transient regime in the present condition. The temperature variation effect on cavity density shown in Table 2 might be, therefore, a temporary effect. Systematic studies on the temperature history effects on the duration of transient regime and the

Table 2
Microstructural parameters obtained by the TEM observation

Materials	Microstructural Parameter	340 °C	225/340 °C
Fe–16Cr–17Ni	Loop density	$2.6 \times 10^{21}/m^3$	$2.4 \times 10^{21}/m^3$
	Cluster density	$1.1 \times 10^{22}/m^3$	$1.6 \times 10^{21}/m^3$
	Cavity size	10 nm	10 nm
	Cavity density	$3.0 \times 10^{19}/m^3$	$1.4 \times 10^{20}/m^3$
V	Cavity size	2.8 nm	1.8 nm
	Cavity density	$1.1 \times 10^{24}/m^3$	$1.4 \times 10^{24}/m^3$
Cu	Void size	60 nm	64 nm
	Void density	$4.0 \times 10^{19}/m^3$	$4.7 \times 10^{19}/m^3$

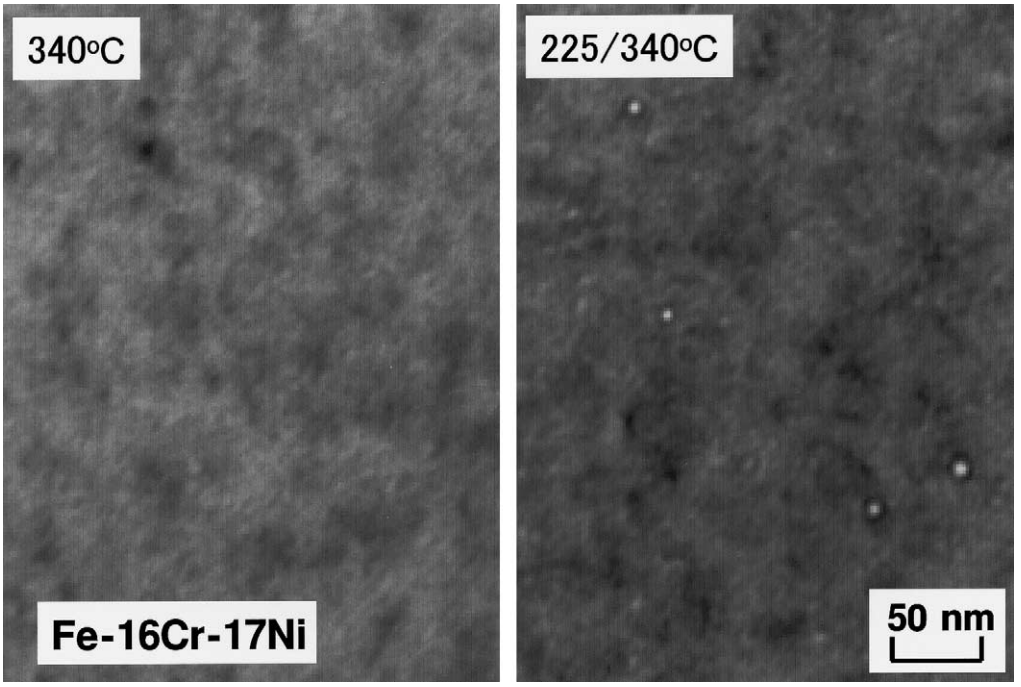

Fig. 5. Comparison of microstructure in a bright field kinematical condition for Fe–16Cr–17Ni induced by 340 °C steady and 225/340 °C variable irradiation. More details of temperature data are available in Fig. 4, Table 1 and [35].

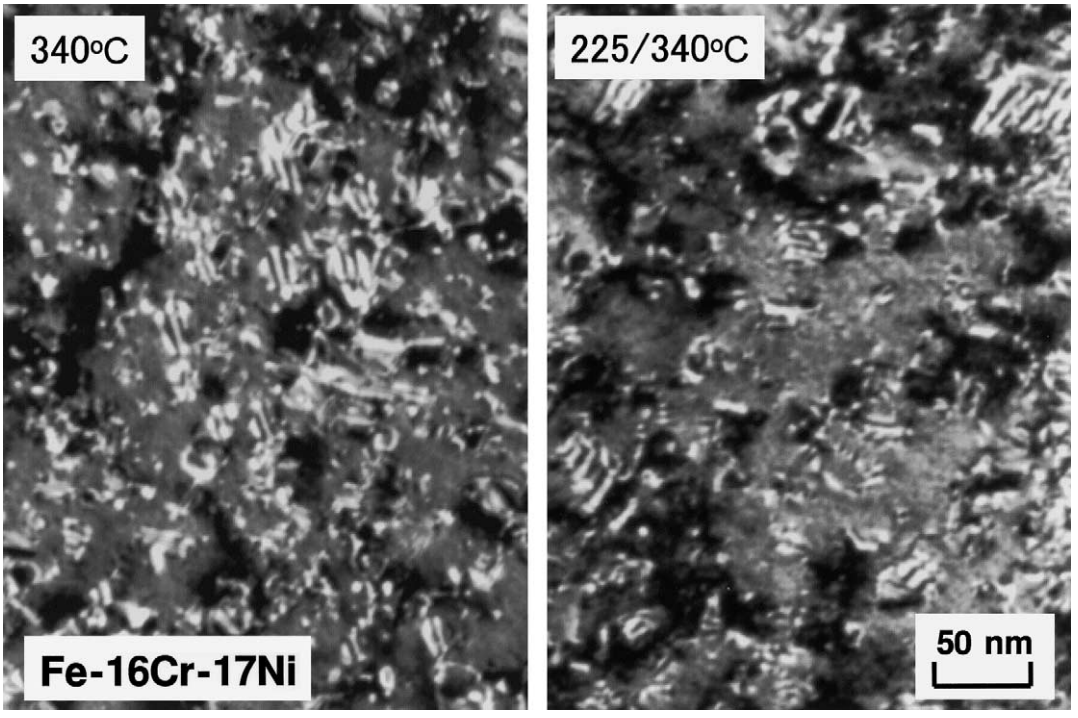

Fig. 6. Same as Fig. 5 except the imaging condition is dark-field weak-beam. Dislocations and small defect clusters are visible as white images.

saturation density are necessary for overall understanding.

3.2. Unalloyed vanadium and V–4Cr–4Ti

In unalloyed vanadium a low density of dislocations and a high density of small cavities were observed for both 340 °C constant and 225/340 °C variable irradiation conditions. The size of the cavities in the variable case is slightly smaller than that in the constant case.

Fig. 7 compares bright-field and weak-beam dark-field images. Thin and long plate-shaped precipitates were observed in the variable cases in both the bright and dark field images. They are oriented in ⟨100⟩ directions. An ion irradiation study of the same material [19] showed similar precipitation by irradiation between 500 and 600 °C. The precipitates, however, disappeared with subsequent ion irradiation at 200 °C. Thus their stability under irradiation is believed to be low. Therefore, it may be premature to conclude that the precipitates observed in the present study were formed because of the negative temperature excursion effects.

In V–4Cr–4Ti, high densities of defect clusters were observed in weak beam dark-field imaging conditions in both 340 °C constant and 225/340 °C variable irradiation conditions. They are considered to be a mixture of defect clusters and precipitates as reported in V–Cr–Ti alloys irradiated at 200–400 °C [41–44].

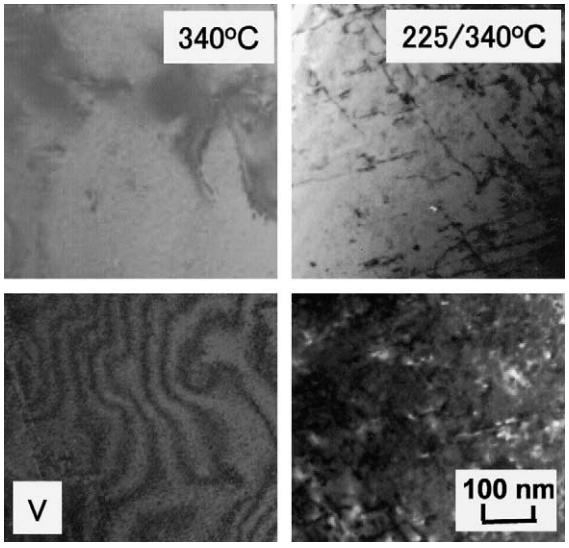

Fig. 7. Comparison of microstructure in bright field kinematical (upper) and dark-field weak-beam imaging (lower) conditions for unalloyed vanadium induced by 340 °C steady and 225/340 °C variable irradiation. More details of temperature data are available in Fig. 4, Table 1 and [35].

3.3. Unalloyed copper

Fig. 8 shows the comparison of microstructures in unalloyed copper in 340 °C constant and 225/340 °C

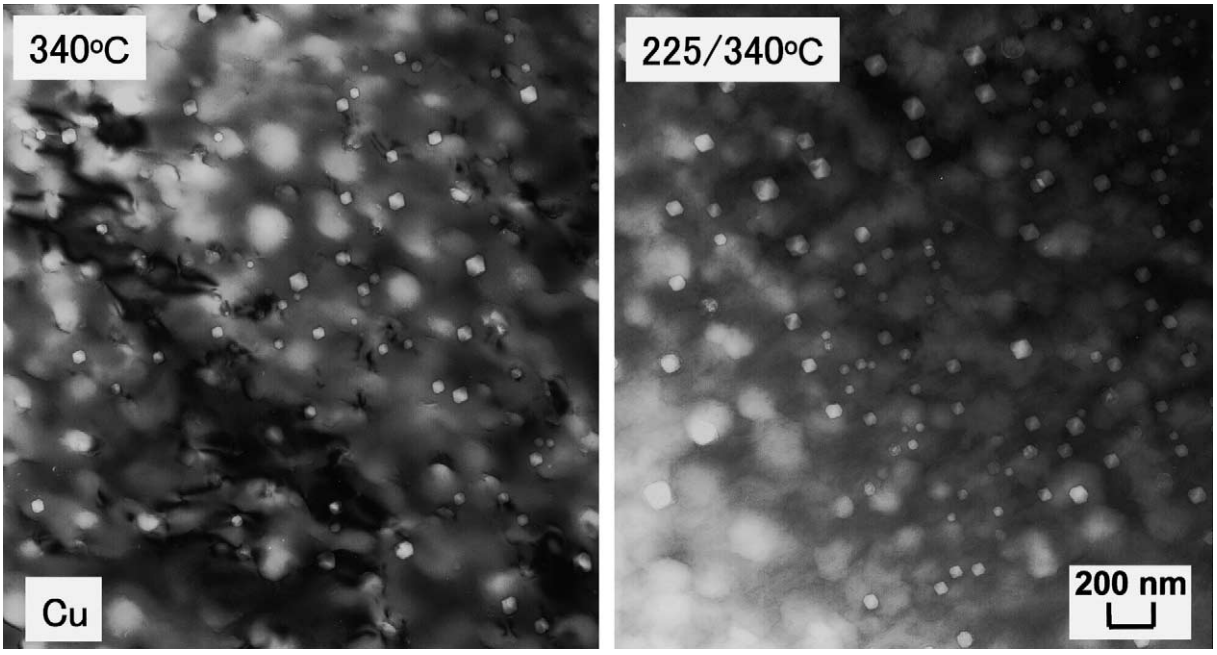

Fig. 8. Comparison of microstructure in bright field kinematical conditions for unalloyed copper induced by 340 °C steady and 225/340 °C variable irradiation. More details of temperature data are available in Fig. 4, Table 1 and [35].

variable irradiation conditions. Voids were formed homogeneously in the matrix, and a low density of tangled dislocations was also formed. Microstructural images in weak-beam conditions showed that the densities of small defect clusters, such as SFT, were low and $<10^{19}$ m^{-3}.

In the present study, no significant difference in microstructure was found between isothermal and temperature-variant irradiation. In the comparison of conventional (includes negative temperature deviation) and improved irradiation in JMTR, enhanced void formation was observed for negative temperature transient at the irradiation temperature of 400 °C but not at 300 °C [3]. Thus the defect processes in the present combination of 200/350 °C in HFIR is considered to be qualitatively similar as those in the conventional control at 300 °C in JMTR.

4. Summary

The varying temperature irradiation experiment conducted in HFIR as part of the Japan–USA Fusion Cooperation Program (JUPITER project) is providing valuable information on the influence of temperature variation at relatively high fluence levels. Post-irradiation examination being actively carried out both by Japanese and US participants will further enhance our understanding of the temperature transient effects on defect processes, microstructural evolution and materials performance.

Acknowledgements

This work was supported by the Japan–USA Fusion Cooperation Program (JUPITER project) sponsored by the Japanese Ministry of Education, Culture, Sports, Science and Technology, and the US Department of Energy. It was sponsored in part by the Office of Fusion Energy Science, US Department of Energy under contract DE-AC05-000R22725 with UT-Battelle, LLC. The authors are thankful to Dr F.W. Wiffen (former US-DOE, presently a Visiting Professor of National Institute for Fusion Science) for reviewing the manuscript.

References

[1] M. Kiritani, J. Nucl. Mater. 160 (1988) 135.
[2] M. Kiritani, T. Yoshiie, S. Kojima, Y. Satoh, K. Hamada, J. Nucl. Mater. 174 (1990) 327.
[3] M. Kiritani, T. Endoh, K. Hamada, T. Yoshiie, A. Okada, S. Kojima, Y. Satoh, H. Kayano, J. Nucl. Mater. 179–181 (1991) 1104.
[4] N. Yoshida, Q. Xu, H. Watanabe, T. Muroga, M. Kiritani, J. Nucl. Mater. 191–194 (1992) 1114.
[5] H. Matsui, K. Kuji, M. Hasegawa, A. Kimura, J. Nucl. Mater. 212–215 (1994) 784.
[6] N. Sekimura, K. Hamada, S. Ishino, ASTM-STP 1175 (1993) 992.
[7] F.A. Garner, N. Sekimura, M.L. Grossbeck, A.M. Ermi, J.W. Newkirk, H. Watanabe, M. Kiritani, J. Nucl. Mater. 205 (1993) 206.
[8] H. Watanabe, T. Muroga, N. Yoshida, J. Nucl. Mater. 217 (1994) 178–186.
[9] T. Muroga, S. Ohnuki, F.A. Garner, S.J. Zinkle, J. Nucl. Mater. 258–263 (1998) 130.
[10] M. Matsuda, N. Yoshida, T. Muroga, M. Kiritani, J. Nucl. Mater. 179–181 (1991) 962.
[11] N. Yoshida, Q. Xu, H. Watanabe, Y. Miyamoto, T. Muroga, J. Nucl. Mater. 212–215 (1994) 471.
[12] M. Kiritani, T. Yoshiie, M. Iseki, S. Kojima, K. Hamada, M. Horiki, Y. Kizuka, H. Inoue, T. Tada, Y. Ogasawara, J. Nucl. Mater. 212–215 (1994) 241.
[13] R. Kasada, A. Kimura, H. Matsui, M. Hasegawa, M. Narui, J. Nucl. Mater. 271&272 (1999) 360.
[14] N. Nita, K. Fukumoto, A. Kimura, H. Matsui, J. Nucl. Mater. 271&272 (1999) 365.
[15] M. Horiki, T. Yoshiie, Q. Xu, M. Iseki, M. Kiritani, J. Nucl. Mater. 283–287 (2000) 282.
[16] D.J. Mazey, T.M. Williams, D.E.J. Bolster, J. Nucl. Mater. 154 (1988) 186.
[17] Q. Xu, H. Watanabe, T. Muroga, N. Yoshida, J. Nucl. Mater. 212–215 (1994) 258.
[18] Q. Xu, H. Watanabe, N. Yoshida, J. Nucl. Mater. 233–237 (1996) 1057.
[19] K. Ochiai, H. Watanabe, T. Muroga, N. Yoshida, H. Matsui, J. Nucl. Mater. 271–272 (1998) 376.
[20] H. Watanabe, T. Arinaga, K. Ochiai, T. Muroga, N. Yoshida, J. Nucl. Mater. 283–287 (2000) 286.
[21] T. Nita, T. Iwai, K. Fukumoto, H. Matsui, J. Nucl. Mater. 283–287 (2000) 291.
[22] D. Hamaguchi, H. Watanabe, T. Muroga, N. Yoshida, J. Nucl. Mater. 283–287 (2000) 319.
[23] M. Kiritani, K. Urban, N. Yoshida, Radiat. Eff. 61 (1981) 117.
[24] T. Muroga, Y. Nonaka, N. Yoshida, J. Nucl. Mater. 233–237 (1996) 1035.
[25] S. Watanabe, J. Satou, N. Sakaguchi, H. Takahashi, C. Namba, J. Nucl. Mater. 239 (1996) 200.
[26] R. Kasada, A. Kimura, J. Nucl. Mater. 283–287 (2000) 188.
[27] Q. Xu, H.L. Heinisch, T. Yoshiie, J. Nucl. Mater. 283–287 (2000) 297.
[28] Y. Katoh, R.E. Stoller, A. Kohyama, T. Muroga, J. Nucl. Mater. 283–287 (2000) 313.
[29] K. Abe, A. Kohyama, C. Namba, F.W. Wiffen, R.H. Jones, J. Nucl. Mater. 258–263 (1998) 2075.
[30] A.L. Qualls, T. Muroga, Fusion Materials Semiannual Progress Report for Period Ending December 31, 1996, DOE/ER-0313/21, p. 255.
[31] A.L. Qualls, M.T. Hurst, D.G. Raby, D.W. Sparks, T. Muroga, Fusion Materials Semiannual Progress Report for Period Ending June 30, 1997, DOE/ER-0313/22, p. 243.
[32] A.L. Qualls, T. Muroga, J. Nucl. Mater. 258–263 (1998) 407.

[33] A.L. Qualls, R.G. Sitterson, Fusion Materials Semiannual Progress Report for Period Ending June. 30, 1998, DOE/ER-0313/24, p. 260.
[34] A.L. Qualls, T. Muroga, Fusion Materials Semiannual Progress Report for Period Ending December 31, 1998, DOE/ER-0313/25, p. 302.
[35] A.L. Qualls, T. Muroga, Fusion Materials Semiannual Progress Report for Period Ending June 30, 2000, DOE/ER-0313/28, p. 266.
[36] T. Muroga, N. Yoshida, J. Nucl. Mater. 212–215 (1994) 266.
[37] S.J. Zinkle, N. Hashimoto, D.T. Hoelzer, A.L. Qualls, T. Muroga, Fusion Materials Semiannual Progress Report for Period Ending December 31, 2000, DOE/ER-0313/29, pp. 162–167.
[38] T. Muroga, K. Araki, Y. Miyamoto, N. Yoshida, J. Nucl. Mater. 155–157 (1988) 1118.
[39] T. Muroga, H. Watanabe, N. Yoshida, J. Nucl. Mater. 212–215 (1994) 482.
[40] S.J. Zinkle, P.J. Maziasz, R.E. Stoller, J. Nucl. Mater. 206 (1993) 266.
[41] D.S. Gelles, P.M. Rice, S.J. Zinkle, H.M. Chung, J. Nucl. Mater. 258–263 (1998) 1380.
[42] D.S. Gelles, J. Nucl. Mater. 283–287 (2000) 344.
[43] P.M. Rice, S.J. Zinkle, J. Nucl. Mater. 258–263 (1998) 1414.
[44] D.T. Hoelzer, S.J. Zinkle, Fusion Materials Semiannual Progress Report for Period Ending December 31, 2000, DOE/ER-0313/29, p. 19.